John von Neumann Institute for Computing

Modelling of Atmospheric Chemistry-Transport Processes

Ralf Wolke, Oswald Knoth, Eberhard Renner,
Wolfram Schröder, Jörg Weickert

published in

NIC Symposium 2001, Proceedings,
Horst Rollnik, Dietrich Wolf (Editor),
John von Neumann Institute for Computing, Jülich,
NIC Series, Vol. **9**, ISBN 3-00-009055-X, pp. 453-462, 2002.

http://www.fz-juelich.de/nic-series/volume9

Modelling of Atmospheric Chemistry-Transport Processes

Ralf Wolke[1], **Oswald Knoth**[1], **Eberhard Renner**[1], **Wolfram Schröder**[1], **and Jörg Weickert**[1]

Institute for Tropospheric Research
Permoserstr. 15, 04303 Leipzig, Germany
E-mail: wolke@tropos.de

Air quality models base on mass balances described by systems of time-dependent, three-dimensional advection-diffusion-reaction equations. To date, one limitation of schemes for the numerical solution of such systems has been their inability to solve equations both quickly and with a high accuracy in multiple grid cell models. This requires the use of fast parallel computers. Multiblock grid techniques and implicit-explicit (IMEX) time integration schemes are suited to take benefit from the parallel architecture. A parallel version of the multiscale chemistry-transport code MUSCAT is presented which is based on these techniques. The meteorological fields are generated simultaneously by the non-hydrostatic meteorological model LM. Both codes run in parallel mode on a predefined number of processors and exchange informations by an implemented coupler interface. The ability and performance of the model system are discussed.

1 Introduction

Atmospheric chemistry-transport models are useful tools for the understanding of pollutant dynamics in the atmosphere. Such air quality models are numerically expensive in terms of computing time. This is due to the fact that their resulting systems of ordinary differential equations (ODE) are nonlinear, highly coupled and extremely stiff. In chemical terms, a stiff system occurs when the lifetime of some species are many orders of magnitude smaller than the lifetime of other species. To illustrate the magnitude of the problem, we note that the stiffness ratio for a typical tropospheric photo-chemistry system is usually greater than 10^{10}. Because explicit ODE solvers require numerous short time steps in order to maintain stability, most current techniques solve stiff ODEs implicitly or by implicit-explicit schemes.

For our air quality studies, the chemistry-transport-model MUSCAT (**MU**ilti**S**cale **C**hemistry **A**erosol **T**ransport) has been utilized[12,6]. The code is parallelized and is tested on several computer systems. Presently, MUSCAT has an online-coupling to the parallel, non-hydrostatic meteorological code LM[1,8] which is the operational regional forecast model of the German Weather Service. Both parallel codes work on their own predefined fraction of the available processors and have their own separate time step size control, see Fig. 1. The coupling scheme simultaneously provides time-averaged wind fields and time-interpolated values of other meteorological fields (vertical exchange coefficient, temperature, humidity, density). Coupling between meteorology and chemistry-transport takes place at each horizontal advection time step only. This scheme can easily be extended to the coupling of MUSCAT with other mesoscale meteorological codes. In the previous version of our model system, it was used for the coupling of the parallel MUSCAT to the mesoscale model METRAS[9]. This meteorological model is also a non-hydrostatic model developed for regional applications. In this version, METRAS runs only on one processor.

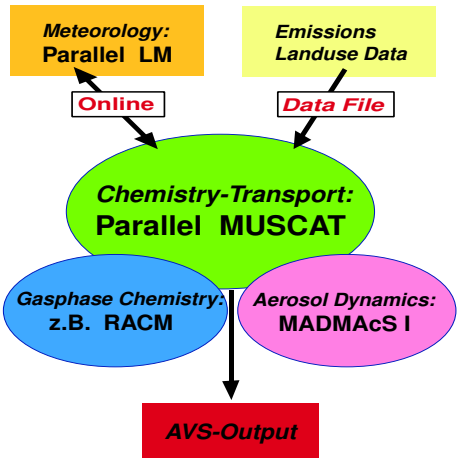

Figure 1. The coupled model system LM–MUSCAT.

In MUSCAT, the horizontal grid is subdivided into so-called *"blocks"*. The code is parallelized by distributing these blocks on the available processors. This may lead to load imbalances, since each block has its own time step size control defined by the implicit time integrator. Therefore, well-suited dynamic load balancing is proposed and investigated. In Sec. 5 the benefit of a developed strategy is discussed for a "Berlioz" ozone scenario. Finally, the ability of MUSCAT for environmental studies is demonstrated for the "Black Triangle" area.

2 The Chemistry-Transport Code MUSCAT

Air quality models base on mass balances described by systems of time-dependent, three-dimensional advection-diffusion-reaction equations

$$\frac{\partial y}{\partial t} + \frac{\partial}{\partial x_1}(u_1 y) + \frac{\partial}{\partial x_2}(u_2 y) + \frac{\partial}{\partial x_3}(u_3 y) = \frac{\partial}{\partial x_3}(\rho K_z \frac{\partial y/\rho}{\partial x_3}) + Q + R(y). \quad (1)$$

y denotes a vector of species concentrations or aerosol characteristics which will be predicted and ρ is the density of the air. The wind field (u_1, u_2, u_3) and the vertical diffusion coefficient K_z are computed simultaneously by a meteorological model. The conversion term R represents the atmospheric chemical reactions and / or the aerosol-dynamical processes. Q denotes prescribed time-dependent emissions.

Multiblock Grid. In MUSCAT a static grid nesting technique[12,6] is implemented. The horizontal grid is subdivided into so-called *"blocks"*. Different resolutions can be used for individual subdomains in the multiblock approach, see Fig. 2. This allows fine resolution for the description of the dispersion in urban regions and arround large point sources. The multiblock structure originates from dividing an equidistant horizontal grid (usually the meteorological grid) into rectangular blocks of different size. By means of doubling or halving the refinement level, each block can be coarsened or refined separately. This is done on condition that the refinements of neighbouring blocks differ by one level at the

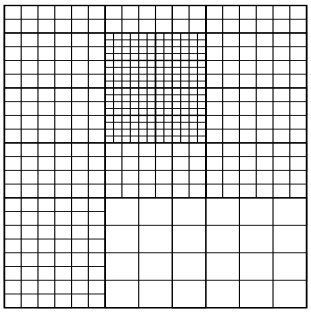

Figure 2. Multiblock grid.

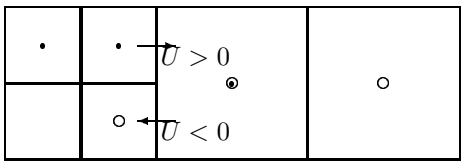

Figure 3. Stencil for advection operator at the interface between different resolutions. • for $U > 0$, ○ for $U < 0$.

most. The maximum size of the already refined or coarsened blocks is limited by a given maximum number of columns. The vertical grid is the same as in the meteorological model.

The spatial discretization is performed by a finite-volume scheme on a staggered grid. We implemented a first order upwind and a biased upwind third order procedure with additional limiting[3]. This scheme has to be applied to non-equidistant stencils which occur at the interface of blocks with different resolutions[6]. Fig. 3 illustrates the choice of the grid values involved in the interpolation formula for the two different upstream directions. In this case the grid cell has five cell wall interfaces.

Time Integration. For the integration in time of the spatially discretized equation (1) we apply an IMEX scheme[12]. This scheme uses explicit second order Runge-Kutta methods for the integration of the horizontal advection and an implicit method for the rest. The fluxes resulting from the horizontal advection are defined as a linear combination of the fluxes from the current and previous stages of the Runge-Kutta method. These horizontal fluxes are treated as "artificial" sources within the implicit integration. Within the implicit integration, the stiff chemistry and all vertical transport processes (turbulent diffusion, advection, deposition) are integrated in a coupled manner by the second order BDF method. We apply a modification of the code LSODE[2] with a special linear system solver. The error control can lead to several implicit time steps per one explicit step. Furthermore, different implicit step sizes may be generated in different blocks. The "large" explicit time step is chosen as a fraction of the CFL number. Higher order accuracy and stability conditions for this class of IMEX schemes are investigated in Knoth and Wolke[5].

Gas Phase Chemistry. The chemical reaction systems are given in ASCII data files in a notation that is easily understandable. For the task of reading and interpreting these chemical data we have developed a preprocessor. Contained in its output file are all data structures required for the computation of the chemical term $R(y)$ and the corresponding Jacobian. Changes within the chemical mechanism or the replacement of the whole chemistry can be performed in a simple and comprehensive way. Several gas phase mechanisms (e.g. RACM, RADM2, CBM IV) are used successfully in 3D case studies. Time resolved anthropogenic emissions are included in the model via point, area and line sources. It is distinguished between several emitting groups. Biogenic emissions are parameterized in terms of land use type, temperature and radiation.

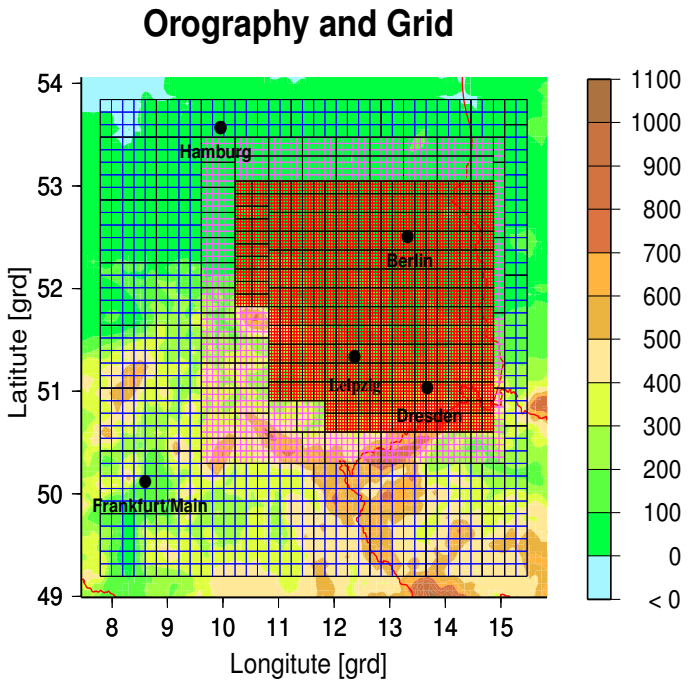

Figure 4. Orography and multiblock grid for the Berlioz simulation.

Aerosol Dynamics. For simulation of aerosol-dynamical processes the model MADMAcS I[11] was included in MUSCAT. The particle size distribution and the aerosol-dynamical processes (condensation, coagulation, sedimentation and deposition) are described using the modal technique. The mass fractions of all particles within one mode are assumed to be identical. Particle size distribution changes owing to various mechanisms, which are divided into external processes like particle transport by convection and diffusion, deposition and sedimentation as well as internal processes like condensation, evaporation, homogeneous nucleation and coagulation.

Parallelization. Our parallelization approach is based on the distribution of blocks among the processors. Inter-processor communication is realized by means of MPI. The exchange of boundary data is organized as follows. Since the implicit integration does not treat horizontal processes, it can be processed in each column separately, using its own time step size control. An exchange of data over block boundaries is necessary only once during each Runge-Kutta substep. Each block needs the concentration values in one or two cell rows of its neighbours, according to the order of the advection scheme. The implementation of the boundary exchange is not straightforward because of the different resolutions of the blocks. The possibilities of one cell being assigned to two neighbouring cells or of two cells receiving the same value must be taken into account. We apply the technique of "extended arrays": the blocks use additional boundary stripes on which incoming data of neighbouring blocks can be stored. Hence, each processor only needs memory for the data of blocks that are assigned to it.

3 Online-Coupling to the Parallel Meteorological Model LM

In Wolke and Knoth[12] an online-coupling technique between the chemistry-transport code MUSCAT and the mesoscale non-hydrostatic meteorological model METRAS (Schlünzen, 1990) is proposed. The meteorological and the chemistry-transport algorithms have their own separate time step size control. The coupling procedure is adapted to the applied IMEX schemes in the chemistry-transport code. All meteorological fields are given with respect to the equidistant horizontal meteorological grid. They have to be averaged or interpolated from the base grid into the block-structured chemistry-transport grid with different resolutions. The velocity field is supplied by its normal components on the faces of each grid cell, and their corresponding contravariant mass flux components fulfill a discrete version of the continuity equation in each grid cell. This property has to be preserved for refined and coarsened cells. Because only the mass flux components are needed for the advective transport of a scalar, the necessary interpolation is carried out for these values. The interpolation is done recursively starting from the meteorological level.

The same approach is applied to the coupling with the meteorological driver LM. Since LM solves a compressible version of the model equations an additional adjustment of the meteorological data is necessary. The velocity components are projected such that a discrete version of the continuity equation is satisfied. The main task of this projection is the solution of an elliptic equation by a preconditioned conjugate gradient method. This is also done in parallel on the LM processors. The projected wind fields and the other meteorological data are gathered by one of the LM processors. This processor communicates directly with each of the MUSCAT processors.

4 Parallel Performance and Load Balancing

In this section, the parallel performance and the run time behaviour of the model system is discussed for a typical meteorological "summer smog" situation ("Berlioz ozone scenario"). In the following we focus on the computational aspects. A discussion of the simulation from an environmental point of view would go beyond the scope of this paper.

The model area covers approximately 640 km x 640 km with a multiscale grid with resolutions of about 4 km–8 km–16 km, see Fig. 4. In the vertical direction the model domain is divided into 19 non-equidistant layers between the surface and a height of approximately 3000 m. The used chemical mechanism RACM[10] considers 73 species and 237 reactions. Time-dependent emission data from both point and area sources are taken into account.

All tests are run on a Cray T3E with various numbers of processors. In all cases, 20 % of the available processors are used for the meteorological code LM, the others for MUSCAT. The equidistant meteorological grid is decomposed into several subdomains whose number corresponds to the number of LM processors. The MUSCAT runs are performed with two different prescribed error tolerances Tol of the BDF integrator.

Dynamical Load Balancing. Consider a static partition where the blocks are distributed between the processors only once at the beginning of the program's run time. Here, we use the number of horizontal cells (i.e., of columns) as measure of the work load of the respective block. Therefore, the total number of horizontal cells of each processor is to be balanced. This is achieved by the grid-partitioning tool *ParMETIS*[4]. It optimizes

both the balance of columns and the “edge cut”, i.e., it takes care for short inter-processor border lines.

In order to improve the load balance, techniques allowing for redistribution of blocks have been implemented. A block’s work load is estimated using the numbers of Jacobian and function evaluations applied during a past time period. According to the work loads of the blocks, ParMETIS searches for a better distribution, besides minimizing the movements of blocks. The communication required for the exchange of block data can be done by means of similar strategies as for the boundary exchange.

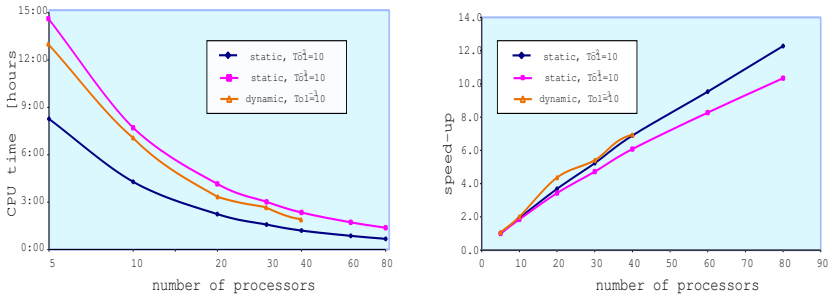

Figure 5. CPU times and speed-up on the Cray T3E.

Performance and Scalability. In the three cases, only the work load of the MUSCAT processors is changed by the step size control and by the dynamic load balancing procedure. The run time behaviour of the LM processors differs only in their idle times (see also Fig. 6). The parallel performance of the model runs is presented in Fig. 5. In the figure with CPU times, a logarithmic scale is used for the ”number of processor” axis. Higher accuracy requirements increase the work load needed for the implicit integration in MUSCAT significantly. By using dynamic load balancing the CPU times can be reduced by a factor of about 0.8–0.9 in comparison to the static grid decomposition. The speed-up is defined with respect to the runs with 5 processors. For $Tol = 10^{-3}$ we take the dynamic case as reference case. An optimal speed up is reached if the CPU curves show a linear

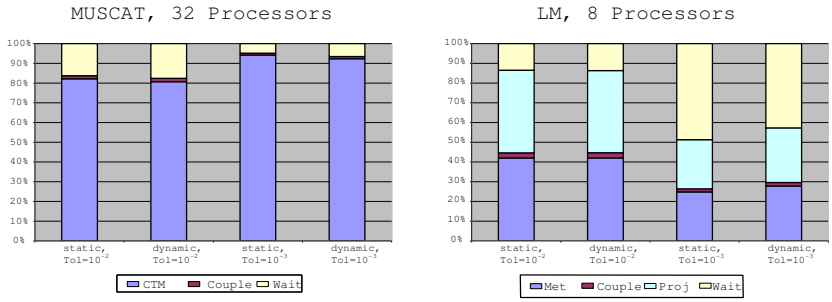

Figure 6. Analysis of the required CPU time for runs with 40 processors.

behaviour with slop one. The measured speed-up values show that the code is scalable up to 80 processors.

The computational behaviour for the 40 processor run is presented in more detail in Fig. 6. In all cases the amount for coupling is negligible. As expected, the idle times of the LM processors growth if the work load of the MUSCAT processors caused by tighter tolerances is increased. Therefore, the number of LM processors can be reduced especially in the runs with higher accuracy. However, the basic strategy consists in the avoidance of idle times on the MUSCAT processors side. The costs for the projection of the wind fields are comparable with that of the LM computations. But it seems that this work load can be reduced by more suitable termination criteria of the cg-method.

5 Air Quality Applications for the "Black Triangle Area"

The "Black Triangle" area has been one of the most polluted areas in middle Europe. Changes in the political situation have altered the emission situation as well and, therefore, also air quality. These changes in air pollution have been investigated and monitored using the previous version METRAS–MUSCAT of the model system. Relevant limit values for protection of human health defined or suggested in directives by the European Commission were checked in worst case scenarios for the year 2005. The species sulfur dioxide, ozone, and aerosol particles have been studied[7]. In the following only a summary of the sulfur dioxide and aerosol particle results is presented.

The model area covers Southern Saxony, Northern Bohemia and parts of Western Poland. As horizontal resolution, 2 km has been chosen. In the vertical, a non-equidistant grid with 27 layers has been used (model top at about 8 km height).

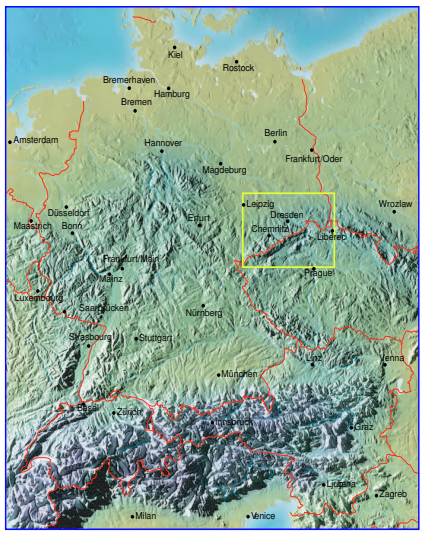

Figure 7. "Black Triangle" area and surrounding regions (yellow box) as used in the model.

The model results have been evaluated for the general pollutant situation for past (1996) and future (2005) emission scenarios as well as in terms of the contributions of several emission source types to the total pollution. For the future scenarios it has been checked if the relevant EU guidelines will possibly be met or under which conditions they can be fulfilled. The anthropogenic emission data base refers to 1996, later scenarios have been estimated using trend factors and information about developments in industry. The data are sorted after emission source types such as households, industry, traffic, and power plants.

Sulfur Dioxide. The simulations have been carried out for meteorological conditions where high values of SO2 concentrations typically occur. In the example below winter high

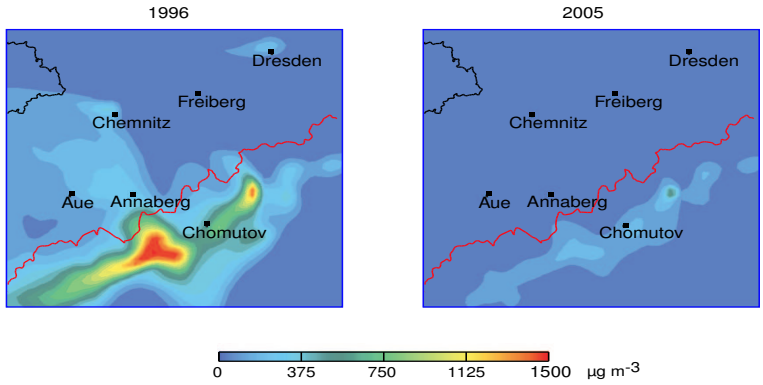

Figure 8. Daily mean values of SO2 concentrations in the lowest model layer.

pressure conditions with moderate winds from the east, ground temperatures of about -6^o C and a strong inversion have been prescribed. Sulfur dioxide is mainly emitted by large power plants (point sources), smaller industrial complexes and coal fires from households. Emissions have been reduced considerably in the last years due to desulfurization and changes in heating systems. The most striking improvement has taken place between 1996 and 1998.

In 1996 high SO2 concentrations mainly originate from emissions of large power plants in Northern Bohemia. Large amounts of SO2 can be transported over wide distances and also into Saxony. Due to the complex topography of the mountain ridge "Erzgebirge" and the position of the major sources, some regions e.g. around Annaberg are more affected than others. Households and small industrial complexes contribute to SO2 pollution to a lesser extent and only very locally around the source areas. Extensive emission reduction particularly at the power plants lead to a major improvement in air quality especially between 1996 and 1998 (not shown).

The relevant EU guideline prescribes for SO2 a 24-hour limit value of 125 μgm^{-3} for the protection of human health, that should not be exceeded more than three days times a calendar year. The simulations for the year 2005 show, that even for assumed worst case meteorological conditions this limit value will be met. So, the pollution due to SO2 should not be of importance for human health in this region for the future.

Aerosols. Particles smaller than PM10 are the relevant part of particulate matter in terms of human health. Recently an EU-guideline for a limit value exists for the mass concentration of the PM 10 fraction only. This part of the total particle emissions has been taken into account in these studies. The resulting amounts have then been distributed into two fractions with two different mean radii as listed in Fig. 9. Particle concentrations in the lowest model layer show similar distributions as sulfur dioxide (winter conditions, winds from the southeast), compare Figs. 11 and 8. From predictions for 2005 it can be concluded that the relevant EU-limit value for the protection of human health (50 μgm^{-3} 8-hour mean value, not more than 35 times a year) can possibly be met even for the assumed worst case meteorological conditions. Some small problems may exist further on near the large power plants in Northern Bohemia.

Emittant group	PM10 mass fraction of emitted particles [%]	% of mass fraction of particles with mean radius of 0.3 µm	% of mass fraction of particles with mean radius of 7.5 µm
power plants a) brown coal b) oil c) gas	 95 75 100	 80 60 100	 15 15 -
other point sources	75	45	30
households	90	80	10
small consumers	75	45	30
traffic	100	100	-

Figure 9. Splitting of the PM 10 emission inventory.

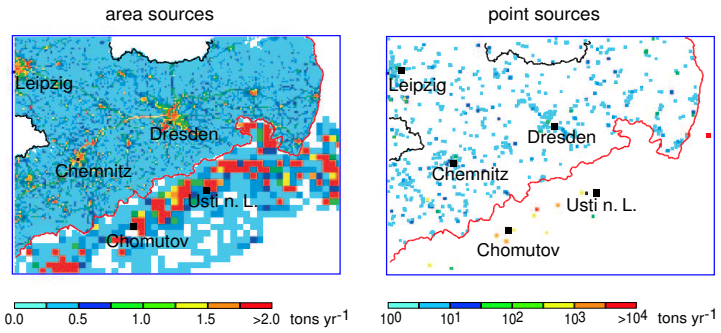

Figure 10. PM 10 emissions 1996.

Conclusions and Outlook

The model system LM–MUSCAT is a powerful instrument for environmental studies. The parallel efficiency is encouraging. In near future, the treatment of cloud chemistry processes will lead to more complex codes. It is well-known that such multiphase processes increases the computational requirements significantly. Furthermore, clouds are dynamic objects with high spatial and temporal variability. Therefore, efficient dynamic load balancing strategies seems to be more important for these simulations.

Acknowledgements

The work was supported by the NIC Jülich, the DFG and the Ministry for Environment of Saxony. Furthermore, we thank the ZHR Dresden and the DWD Offenbach for good cooperation.

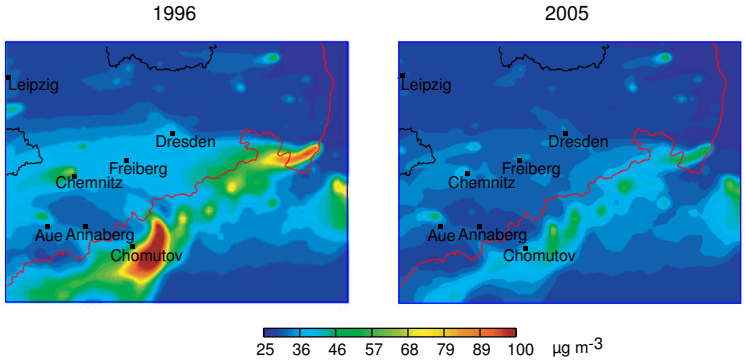

Figure 11. Maximal 8-hour-mean PM 10 concentrations near the ground, 25 $\mu g m^{-3}$ background concentration of PM 10.

References

1. G. Doms and U. Schättler, *The Nonhydrostatic Limited-Area Model LM (Lokal Model) of DWD: I. Scientific Documentation (Version LM-F90 1.35)*, Deutscher Wetterdienst, Offenbach, 1999.
2. A.C. Hindmarsh, *ODEPACK, A systematized collection of ODE solvers*, in Scientific Computing, North-Holland, Amsterdam, 1983, pp. 55-74.
3. W. Hundsdorfer, B. Koren, M. van Loon and J.G. Verwer, *A positive finite-difference advection scheme*, Journal of Computational Physics, 117 (1995), pp. 35-46.
4. G. Karypis, K. Schloegel and V. Kumar, *ParMETIS. Parallel graph partitioning and sparse matrix ordering library. Version 2.0*, University of Minnesota, 1998.
5. O. Knoth and R. Wolke, *Implicit-explicit Runge-Kutta methods for computing atmospheric reactive flow*, Appl. Numer. Math., 28 (1998), pp. 327-341.
6. O. Knoth and R. Wolke, *An explicit-implicit numerical approach for atmospheric chemistry-transport modeling*, Atm. Environ., 32 (1998), pp. 1785-1797.
7. E. Renner, *The Black Triangle area – fit for Europe?*, AMBIO, in press.
8. U. Schättler and G. Doms, *The Nonhydrostatic Limited-Area Model LM (Lokal Model) of DWD: II. Implementation Documentation (Version LM-F90 1.35)*, Deutscher Wetterdienst, Offenbach, 1998.
9. K.H. Schlünzen, *Numerical studies on the inland penetration of sea breeze fronts at a coastline with tidally flooded mudflats*, Beitr. Phys. Atmos., 63 (1990), pp. 243-256.
10. W.R. Stockwell, F. Kirchner, M. Kuhn and S. Seefeld, *A new mechanism for regional atmospheric chemistry modeling*, J. Geophys. Res. D22, 102 (1997), pp. 25847-25879.
11. M. Wilck and F. Stratmann, *A 2-D multicomponent aerosol model and ist application to laminar flow reactors*, J.Aerosol Sci., 28 (1997), pp. 959-972.
12. R. Wolke and O. Knoth, *Implicit-explicit Runge-Kutta methods applied to atmospheric chemistry-transport modelling*, Environmental Modelling and Software, 15 (2000), pp. 711-719.